

# SCIENTIFIC REPORTS



OPEN

## Influence of soil moisture on codenitrification fluxes from a urea-affected pasture soil

Timothy J. Clough<sup>1</sup>, Gary J. Lanigan<sup>2</sup>, Cecile A. M. de Klein<sup>3</sup>, Md. Sainur Samad<sup>4</sup>, Sergio E. Morales<sup>4</sup>, David Rex<sup>1,2</sup>, Lars R. Bakken<sup>5</sup>, Charlotte Johns<sup>1,2</sup>, Leo M. Condrón<sup>1</sup>, Jim Grant<sup>6</sup> & Karl G. Richards<sup>2</sup>

Intensively managed agricultural pastures contribute to N<sub>2</sub>O and N<sub>2</sub> fluxes resulting in detrimental environmental outcomes and poor N use efficiency, respectively. Besides nitrification, nitrifier-denitrification and heterotrophic denitrification, alternative pathways such as codenitrification also contribute to emissions under ruminant urine-affected soil. However, information on codenitrification is sparse. The objectives of this experiment were to assess the effects of soil moisture and soil inorganic-N dynamics on the relative contributions of codenitrification and denitrification (heterotrophic denitrification) to the N<sub>2</sub>O and N<sub>2</sub> fluxes under a simulated ruminant urine event. Repacked soil cores were treated with <sup>15</sup>N enriched urea and maintained at near saturation (−1 kPa) or field capacity (−10 kPa). Soil inorganic-N, pH, dissolved organic carbon, N<sub>2</sub>O and N<sub>2</sub> fluxes were measured over 63 days. Fluxes of N<sub>2</sub>, attributable to codenitrification, were at a maximum when soil nitrite (NO<sub>2</sub><sup>−</sup>) concentrations were elevated. Cumulative codenitrification was higher (P = 0.043) at −1 kPa. However, the ratio of codenitrification to denitrification did not differ significantly with soil moisture, 25.5 ± 15.8 and 12.9 ± 4.8% (stdev) at −1 and −10 kPa, respectively. Elevated soil NO<sub>2</sub><sup>−</sup> concentrations are shown to contribute to codenitrification, particularly at −1 kPa.

The concentration of nitrous oxide (N<sub>2</sub>O) in the atmosphere has increased since 1750 due to human activity with values surpassing the highest concentrations recorded in ice cores during the past 800,000 years, and exceeding the pre-industrial level by 20%<sup>1</sup>. Reductions in the anthropogenic forcing of Earth's climate system and the recovery of the ozone layer would be enhanced if anthropogenic emissions of N<sub>2</sub>O were reduced<sup>1,2</sup>. However, the atmospheric N<sub>2</sub>O concentration continues to increase, predominately due to agricultural intensification, with 80% of the increase resulting from increased fertilizer use and manure applications for the purpose of food production<sup>3</sup>. Nitrous oxide emissions from grazed grasslands make a significant contribution to anthropogenic N<sub>2</sub>O emissions<sup>4,5</sup> as a consequence of ruminant urine patches supplying nitrogen (N) substrate that is in excess of the pasture sward's N requirement<sup>6,7</sup>. Emissions of N<sub>2</sub>O from pastures result from microbial transformations of N substrates applied via nitrification, nitrifier-denitrification, heterotrophic denitrification (hereafter referred to as denitrification unless otherwise stated), and codenitrification<sup>8–10</sup>. A further significant consequence of denitrifying mechanisms is the production and loss of dinitrogen (N<sub>2</sub>). Although environmentally benign, N<sub>2</sub> losses lead to poor N use efficiency and reduced production, resulting in economic losses through the need to add further inorganic N. While reactive N (Nr) losses, such as nitrate (NO<sub>3</sub><sup>−</sup>) leaching and ammonia (NH<sub>3</sub>) volatilization, are well researched, the loss of N<sub>2</sub> from pasture systems is poorly studied and often only identified by default via the application of N balance methods<sup>11</sup>. For example, of the N applied to grasslands some 20–40% is typically unaccounted for and assumed to be lost as N<sub>2</sub><sup>11–13</sup>. Therefore, methods to reduce emissions of both N<sub>2</sub>O and N<sub>2</sub> require a better understanding of the emission pathways.

Shoun *et al.*<sup>14</sup> and Tanimoto *et al.*<sup>15</sup> first described codenitrification after demonstrating, with <sup>15</sup>N tracer, that N<sub>2</sub>O and N<sub>2</sub> production occurred in a different manner to the routinely accepted pathways of nitrification and

<sup>1</sup>Department of Soil and Physical Sciences, Lincoln University, Lincoln, New Zealand. <sup>2</sup>Teagasc, Environmental Research Centre, Johnstown Castle, Wexford, Ireland. <sup>3</sup>AgResearch Invermay, Mosgiel, New Zealand. <sup>4</sup>Department of Microbiology and Immunology, Otago School of Medical Sciences, University of Otago, Dunedin, New Zealand. <sup>5</sup>Department of Environmental Sciences, Norwegian University of Life Sciences, Ås, Norway. <sup>6</sup>Statistics and Applied Physics, Teagasc, Ashtown, Dublin 15, Ireland. Correspondence and requests for materials should be addressed to T.J.C. (email: [Timothy.Clough@lincoln.ac.nz](mailto:Timothy.Clough@lincoln.ac.nz))

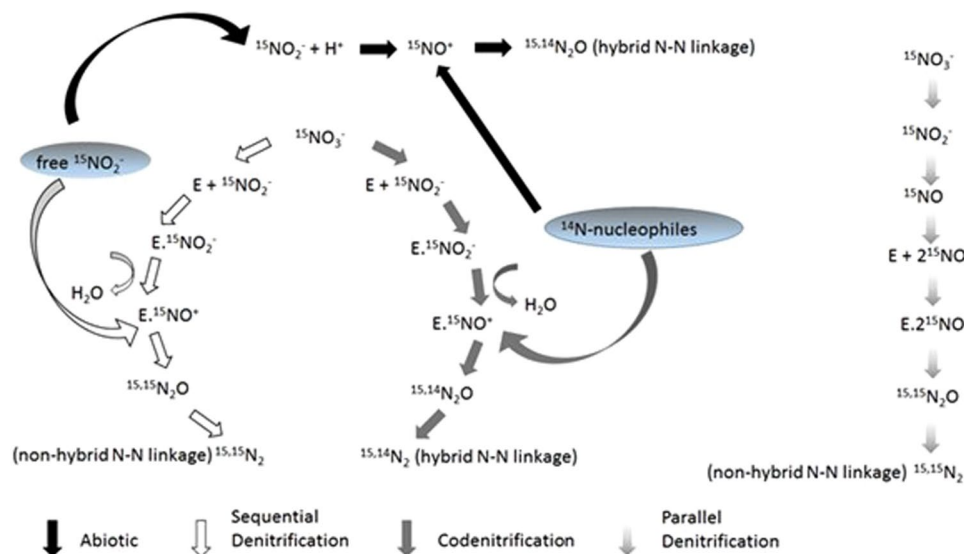


**Figure 1.** Simplified diagram (adapted from Spott *et al.*<sup>16</sup>, Weeg-Aerssens *et al.*<sup>18</sup>, Schmidt *et al.*<sup>55</sup>) showing abiotic denitrification, parallel denitrification, sequential denitrification and codenitrification pathways. During abiotic production an electrophile (e.g. the nitrosonium cation  $\text{NO}^+$  which is formed under acidic soil conditions) replaces the hydrogen atom of a nucleophile with a hybrid N-N bond formed following deprotonation. The parallel pathway results in a non-hybrid N-N bond as the result of two  $\text{NO}_2^-$  or two  $\text{NO}$  molecules being bound, simultaneously to one enzyme (E), which theoretically excludes the possibility of a nitrosation reaction occurring and the formation of a hybrid N-N bond<sup>55,56</sup>. However, a two-step process occurs in the sequential pathway when  $\text{NO}_2^-$  or  $\text{NO}$  molecules initially bind to an enzyme (E) followed by a free  $\text{NO}_2^-$ , or  $\text{NO}$  molecule, (originating from the original  $\text{NO}_3^-$  pool) reacting with the enzyme complexed N species to form a non-hybrid N-N bond. The two-step sequence also permits the enzyme complexed N species to function as an electrophile which is able to be attacked by nucleophiles producing a hybrid N-N bond. Nucleophiles able to partake in codenitrification reactions include amines, ammonium, hydrazine, and ammonia.

denitrification. It has been suggested that codenitrification results from microbially mediated N-nitrosation reactions<sup>14–16</sup>. Codenitrification is one of the least studied N loss pathways and its contribution to agricultural  $\text{N}_2\text{O}$  and  $\text{N}_2$  emissions remains unclear<sup>17</sup>.

Codenitrification is a process that co-metabolises organic N compounds, such as amines, to produce  $\text{N}_2\text{O}$  and/or  $\text{N}_2$ , and is also referred to as biotic N-nitrosation<sup>16</sup>. Codenitrification involves the replacement of a hydrogen atom in an organic compound with a nitroso group ( $-\text{N}=\text{O}$ ). Under near neutral to alkaline soil pH conditions, common to pasture soils, codenitrification may occur via enzymatic catalysis (Fig. 1), with enzymatic nitrosyl compounds ( $\text{E}-\text{NO}^+$  or  $\text{E}-\text{NO}$ ) attracting nucleophilic compounds<sup>16,18</sup>. Nucleophiles involved in codenitrification include hydroxylamine, ammonium ( $\text{NH}_4^+$ ), hydrazine, amino compounds, and ammonia ( $\text{NH}_3$ ). The resulting gas products formed,  $\text{N}_2\text{O}$  or  $\text{N}_2$ , contain one N atom originating from the inorganic-N (e.g.  $\text{NO}_2^-$ ), and a second atom from the co-metabolised organic compound<sup>16,18</sup>. Significant rates of both partial and complete codenitrification are only likely to occur if nucleophile concentrations are at least one or two orders of magnitude greater than that of  $\text{NO}_2^-$  and  $\text{NO}$ <sup>16</sup>.

Heterotrophic denitrification results in the reduction of  $\text{NO}_3^-$  to  $\text{N}_2$  with nitrite ( $\text{NO}_2^-$ ), nitric oxide ( $\text{NO}$ ), and  $\text{N}_2\text{O}$  obligate intermediaries<sup>19</sup> (Fig. 1). Formation of the  $\text{N}_2\text{O}$  molecule is recognized as occurring via parallel or sequential pathways<sup>16</sup> and references therein. In the parallel pathway simultaneous bonding of two  $\text{NO}_2^-$  or two  $\text{NO}$  molecules to an enzyme, where both  $\text{NO}_2^-$  and  $\text{NO}$  are derived from the same  $\text{NO}_3^-$  source, creates a non-hybrid N-N bond, thus precluding the occurrence of codenitrification<sup>16</sup>. However, a two-step reaction, the sequential pathway, results in either  $\text{NO}_2^-$  or  $\text{NO}$  initially bonding with an enzyme, which in turn may react with either free  $\text{NO}_2^-$  or  $\text{NO}$  to form a non-hybrid N-N bond, or alternatively, this enzyme bound N can act as an electrophile and react with nucleophiles (e.g. amines) to form a hybrid N-N bond (Fig. 1). Consequently, hybrid N-N gas production, codenitrification, can occur simultaneously as a result of conventional denitrification (Fig. 1)<sup>16</sup>. Formation of hybrid  $\text{N}_2$  has also been reported to occur when  $\text{NH}_3$ , hydrazine ( $\text{N}_2\text{H}_4$ ) or amines are co-metabolised during codenitrification<sup>20</sup>.

Abiotic nitrosation is also a well-recognized phenomena<sup>21,22</sup>. In abiotic reactions, free  $\text{NO}_2^-$  derived from nitrification or denitrification processes is chemically transformed to produce the nitrosonium cation ( $\text{NO}^+$ ) under acidic conditions. The  $\text{NO}^+$  cation reacts with a nucleophile (e.g. amine) to produce a hybrid N-N linkage (Fig. 1)<sup>16</sup> and references therein. This process differs from codenitrification since the formation of the  $\text{NO}^+$  electrophile is chemically dependent on the soil pH and involves free  $\text{NO}_2^-$  in the soil solution as the precursor. Nucleophiles involved in abiotic reactions include hydroxylamine,  $\text{NH}_4^+$ , hydrazine, amines, and  $\text{NH}_3$ . However, relatively high soil pH values under grazed pasture conditions mean that the equilibrium concentrations of free nitrosating agents are generally inadequate for abiotic nitrosation to be significant<sup>16</sup>.

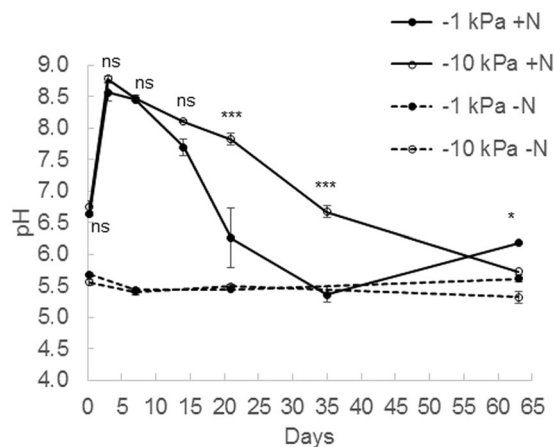


**Figure 2.** Changes in soil pH over time. Soil pH under near saturated (−1 kPa) or field capacity (−10 kPa) soil moisture conditions, following urea application (+N) or nil urea application (−N). Symbols are means ( $n = 4$ ) with vertical error bars the standard error of the mean. Asterisks \*.,\*\*.,\*\*\* indicate significant differences between moisture treatments under urea treatments at  $P < 0.05$ ,  $P < 0.01$ , and  $P < 0.001$ , respectively.

In grazed pastures ruminant urine deposition onto pasture soil temporarily elevates soil pH following urea hydrolysis, creating a urinary-N cascade that produces potential nucleophiles (e.g.  $\text{NH}_4^+$  and  $\text{NH}_3$ ) at high concentrations. Simultaneously, enzyme bound nitrosating agents (E- $\text{NO}^+$  or E- $\text{NO}$ ), may be formed during denitrification of nitrate ( $\text{NO}_3^-$ ) or as supplied by  $\text{NO}_2^-$  or  $\text{NO}$  during processes such as nitrification of nitrifier-denitrification<sup>19</sup>. Thus urine patches are potentially conducive to codenitrification occurring. In the only *in vivo* study to date to focus on codenitrification, Selbie *et al.*<sup>23</sup> confirmed the occurrence of codenitrification within ruminant urine-affected pasture soil with 95% of the  $\text{N}_2$  emitted over 123 days resulting from codenitrification, with  $\text{N}_2$  the dominant product, and where the codenitrified  $\text{N}_2$  was equivalent to 56% of the N applied. This experiment by Selbie *et al.*<sup>23</sup> received regular rainfall and it may be that the dominance of codenitrified  $\text{N}_2$  over codenitrified  $\text{N}_2\text{O}$  may have been the result of, as the authors suggest, hybrid  $\text{N}_2\text{O}$  being converted to hybrid  $\text{N}_2$  via heterotrophic denitrification (Fig. 1). Conceptually, the recognized environmental constraints on denitrification should also apply to codenitrification<sup>16</sup>, since codenitrification depends on enzyme bound nitrosyl compounds, formed during denitrification, being present (Fig. 1). A key driver of denitrification is the soil's oxygen status, and wetter soils result in higher levels of anaerobiosis since oxygen diffuses  $1 \times 10^4$  times slower through water when compared to air<sup>24</sup>. Thus wetter soils should have higher rates of codenitrification. In order to test this hypothesis, and better understand the constraints and importance of codenitrification in pasture soils, we performed an experiment using either saturated soil or soil at field capacity to determine relative rates of codenitrification. The objective of the study was to investigate the effect of soil moisture on the rate of codenitrification from simulated urine applied to a free draining permanent grassland soil.

## Results

**Soil moisture, pH, DOC and inorganic-N.** The −1 kPa and −10 kPa moisture treatments imposed resulted in average WFPS values (% $\pm$ s.e.m) of  $88.9 \pm 1.1$  and  $48.5 \pm 0.4$ , respectively. The relative gas diffusivity values at −1 and −10 kPa were 0.0028 and 0.2079, respectively. There was a significant interaction of soil moisture and sampling date ( $p < 0.001$ ) on soil pH, DOC and inorganic N contents (Figs 2–4). Soil pH in the non-urea treatment was generally constant over time (Fig. 2) regardless of soil moisture treatment, averaging  $5.49 \pm 0.11$  (Stdev). However, soil pH ( $p < 0.001$ ) increased within 6 hours of urea application, and increased further, peaking at  $8.57 \pm 0.29$  and  $8.78 \pm 0.09$  in the −1 kPa and −10 kPa treatments, respectively, on day 3 before declining over time (Fig. 2). On days 21 and 35 the soil pH was lower in the −1 kPa treatment than in the −10 kPa treatment ( $p < 0.001$ ) with the reverse occurring on day 63 ( $p < 0.05$ ).

Soil DOC was higher ( $P < 0.001$ ) under the urea treatment throughout the experiment (Fig. 3) and within the urea treatment soil DOC concentrations were significantly lower at −1 kPa than at −10 kPa from day 3 to day 62 (Fig. 3). In the urea treatment soil DOC correlated strongly with soil pH at both −1 kPa ( $r = 0.79$ ;  $p < 0.001$ ) and −10 kPa ( $r = 0.89$ ;  $p < 0.001$ ).

Soil  $\text{NH}_4^+$ -N concentrations increased following urea application (Fig. 4), peaking at day 3 and then declining over time with a faster rate of decline in the −1 kPa treatment from day 14 ( $p < 0.05$ ) such that soil  $\text{NH}_4^+$ -N concentrations were lower at −1 kPa on days 35 and 63 (Fig. 4). The  $^{15}\text{N}$  enrichment of the  $\text{NH}_4^+$ -N in the urea treatment declined from 44 to 37 atom% over the experiment with higher  $^{15}\text{N}$  enrichment on days 14, 21 and 35 in the −10 kPa treatment (Fig. 5). Concentrations of  $\text{NO}_2^-$ -N increased from day 7 under the urea treatment and peaked at day 21, with more  $\text{NO}_2^-$ -N present in the −1 kPa treatment, prior to returning to background levels at day 35 (Fig. 4). Concentrations of  $\text{NO}_2^-$ -N, extracted from the urea treatment, were only sufficient for  $^{15}\text{N}$  enrichment determinations on days 14 and 21, where the  $^{15}\text{N}$  enrichment was higher ( $p < 0.05$ ) at −1 kPa than at −10 kPa on day 14, with no differences on day 21 (Fig. 5). Soil  $\text{NO}_3^-$ -N concentrations also began to increase at day 7 under the urea treatment and were consistently higher ( $p < 0.001$ ) in the −1 kPa treatment on days 14 and 21. Soil  $\text{NO}_3^-$ -N concentrations peaked on day 35, before they declined to be less than those observed in the

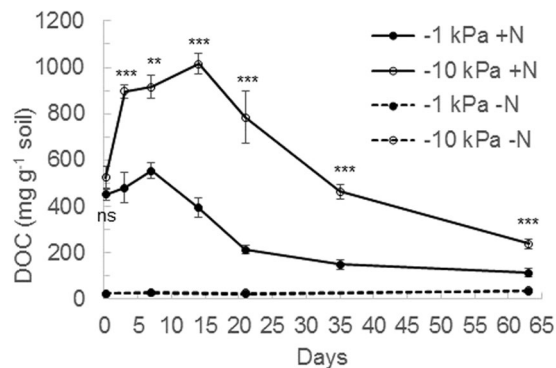


**Figure 3.** Changes in soil cold water extractable organic carbon (DOC) over time. Concentrations of soil DOC under near saturated (−1 kPa) or field capacity (−10 kPa) soil moisture conditions, following urea application (+N) or nil urea application (−N). Symbols are means ( $n = 4$ ) with vertical error bars the standard error of the mean. Asterisks \*\*\*, \*\*, ns indicate significant differences between moisture treatments under urea treatments at  $P < 0.05$ ,  $P < 0.01$ , and  $P < 0.001$ , respectively.

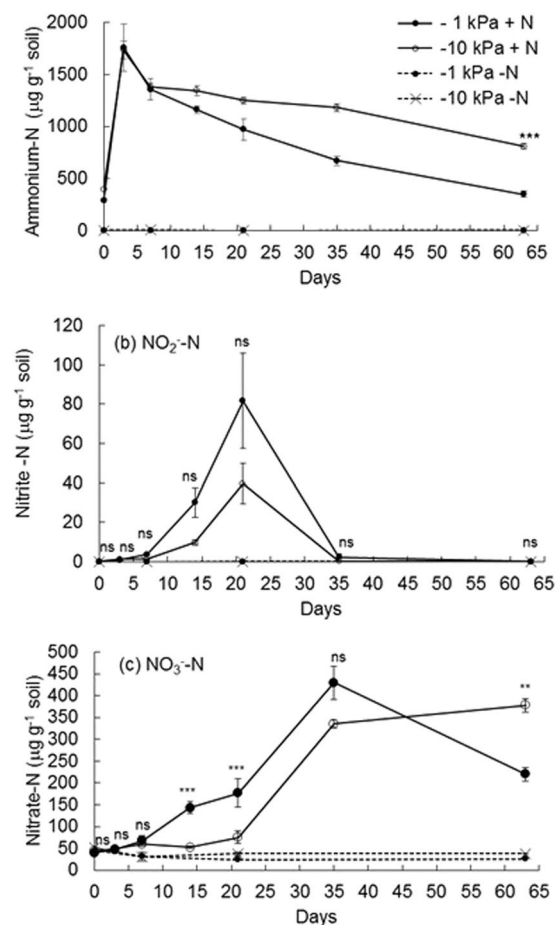


**Figure 4.** Changes in soil inorganic-N over time. Concentrations of extractable (a) ammonium-N (b) nitrite-N and (c) nitrate-N under near saturated (−1 kPa) or field capacity (−10 kPa) soil moisture conditions, following urea application (+N) or nil urea application (−N). Symbols are means ( $n = 4$ ) with vertical error bars the standard error of the mean. Asterisks \*\*\*, \*\*, ns indicate significant differences between moisture treatments under urea treatments at  $P < 0.05$ ,  $P < 0.01$ , and  $P < 0.001$ , respectively.

−10 kPa treatment ( $p < 0.01$ ) at day 63 (Fig. 4). Changes in soil  $\text{NO}_3^-$ - $^{15}\text{N}$  enrichment reflected the concentration dynamics with  $^{15}\text{N}$  enrichment increasing faster at −1 kPa to 41 atom%  $^{15}\text{N}$  at day 21 while at −10 kPa the  $\text{NO}_3^-$ - $^{15}\text{N}$  enrichment was only 34 atom%  $^{15}\text{N}$  by day 63 (Fig. 5).

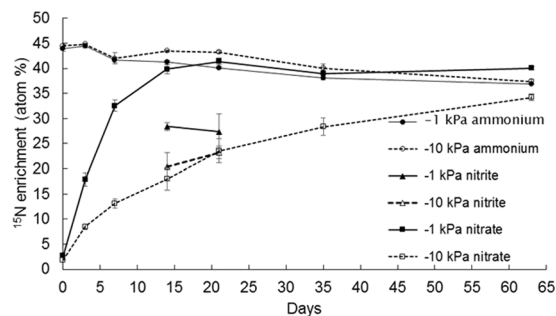


**Figure 5.** Inorganic-N  $^{15}\text{N}$  enrichment over time. The  $^{15}\text{N}$  enrichment of the ammonium-N ( $\text{NH}_4^+\text{-N}$ ), nitrite-N ( $\text{NO}_2^-\text{-N}$ ) and nitrate-N ( $\text{NO}_3^-\text{-N}$ ) are shown over time following  $^{15}\text{N}$  urea application at near saturated ( $-1$  kPa) or field capacity ( $-10$  kPa) soil moisture conditions. Symbols are means ( $n=4$ ) with vertical error bars the standard error of the mean.

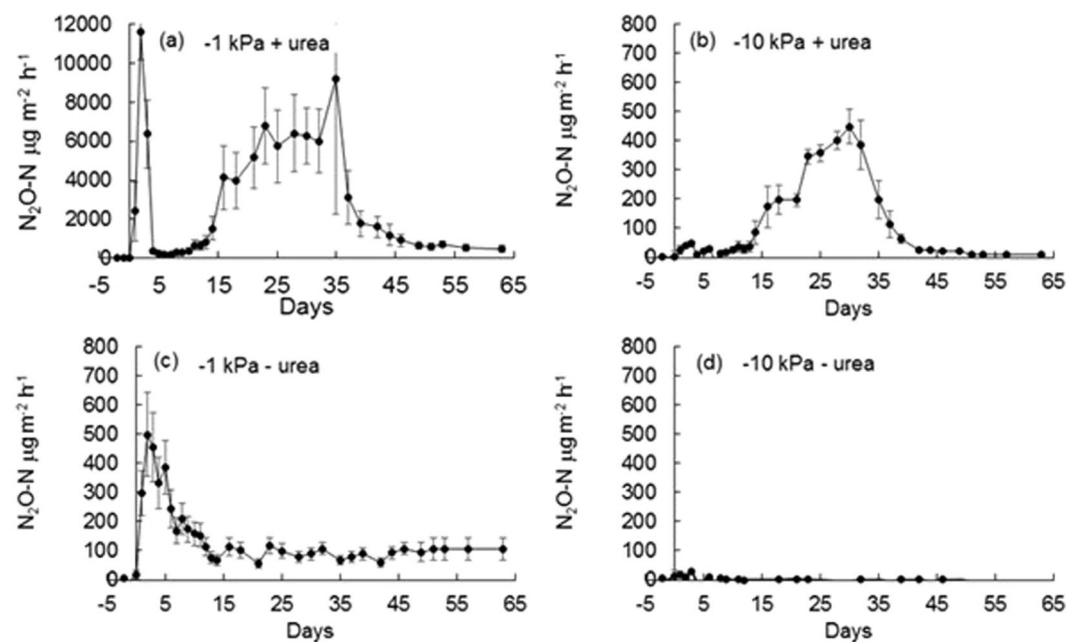


**Figure 6.** Nitrous oxide fluxes over time. Fluxes of  $\text{N}_2\text{O}$  under near saturated ( $-1$  kPa) or field capacity ( $-10$  kPa) soil moisture conditions, following urea application (+N) or nil urea application ( $-N$ ) where (a)  $-1$  kPa +N (b)  $-10$  kPa +N (c)  $-1$  kPa  $-N$  and (d)  $-10$  kPa  $-N$  show  $\text{N}_2\text{O}$  fluxes over time. Note differing y-axis scales. Symbols are means ( $n=4$ ) with vertical error bars the standard error of the mean.

**$\text{N}_2\text{O}$ -N fluxes and  $^{15}\text{N}$  enrichment.** Trends in daily  $\text{N}_2\text{O}$  fluxes differed with treatment (Fig. 6). At  $-10$  kPa in the absence of urea  $\text{N}_2\text{O}$ -N fluxes were generally  $<5 \mu\text{g m}^{-2} \text{h}^{-1}$ , with fluxes only greater than this ( $\leq 29 \mu\text{g m}^{-2} \text{h}^{-1}$ ) between day 0 and day 10 following treatment application (Fig. 6). Under the  $-1$  kPa treatment, in the absence of urea,  $\text{N}_2\text{O}$ -N fluxes also peaked after water application on day 2 at  $498 \mu\text{g m}^{-2} \text{h}^{-1}$ , before declining to ca  $100 \mu\text{g m}^{-2} \text{h}^{-1}$  on day 12, where after  $\text{N}_2\text{O}$ -N fluxes were constant until day 63, averaging  $92 \mu\text{g m}^{-2} \text{h}^{-1}$  between days 12 to 63 (Fig. 6). Adding urea at  $-10$  kPa caused  $\text{N}_2\text{O}$ -N fluxes to increase steadily from day 12 until they peaked at day 30 ( $449 \mu\text{g m}^{-2} \text{h}^{-1}$ ) where after they steadily declined to  $<10 \mu\text{g m}^{-2} \text{h}^{-1}$  by day 51 (Fig. 6). The highest  $\text{N}_2\text{O}$ -N fluxes were observed at  $-1$  kPa with urea addition, where a rapid increase in the flux occurred peaking at  $11,603 \mu\text{g m}^{-2} \text{h}^{-1}$  on day 2, followed by a rapid decrease to  $163 \mu\text{g m}^{-2} \text{h}^{-1}$  by day 7. Then the flux gradually increased until day 35 ( $9220 \mu\text{g m}^{-2} \text{h}^{-1}$ ) whereupon it too decreased to be  $476 \mu\text{g m}^{-2} \text{h}^{-1}$  by day 61 (Fig. 6).

Soil moisture treatment influenced cumulative  $\text{N}_2\text{O}$ -N fluxes ( $p < 0.001$ ) with total emissions of  $0.08$  and  $2.26 \text{ g N}_2\text{O-N m}^{-2}$  at  $-10$  and  $-1$  kPa, respectively, when averaged over plus and minus urea treatments. Similarly, application of urea increased cumulative  $\text{N}_2\text{O}$ -N fluxes ( $p < 0.001$ ) from  $0.10$  to  $2.25 \text{ g N}_2\text{O-N m}^{-2}$  when averaged over soil moisture treatments. An interaction between soil moisture and N application ( $p < 0.002$ ) resulted in higher cumulative  $\text{N}_2\text{O}$ -N fluxes at  $-1$  kPa when urea was applied equal to  $3.99 \text{ g m}^{-2}$  (Table 1). The  $\text{N}_2\text{O}$ -N emission factors for the urea-N applied, allowing for non-N fluxes equated to  $4.14\%$  and  $0.18\%$  of N applied at  $-1$  kPa and  $-10$  kPa, respectively.

Urea-N	Moisture (kPa)	N <sub>2</sub> O		N <sub>2DN</sub>		N <sub>2co</sub>	
+N	-1	3.99	A	8.61	A	1.92	A
+N	-10	0.18	B	1.98	A	0.26	B
-N	-1	0.16	B	na		na	
-N	-10	-0.0003	C	na		na	
P value		0.0321		0.0554		0.0437	

**Table 1.** Mean cumulative N<sub>2</sub>O, N<sub>2DN</sub> and N<sub>2co</sub> emissions (g N m<sup>-2</sup>). P values are for the interaction between treatments. Tukey-Kramer grouping: LS-means with the same letter are not significantly different, na not applicable. N<sub>2DN</sub> and N<sub>2co</sub> represent heterotrophic denitrification and codenitrification, respectively.

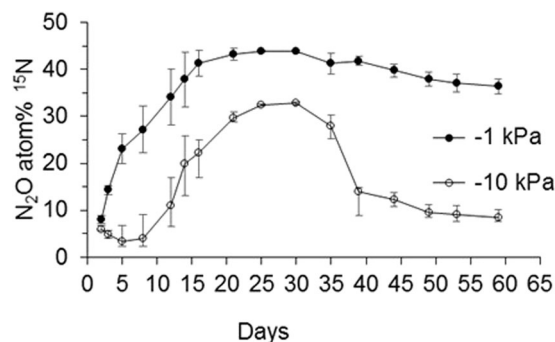


**Figure 7.** Nitrous oxide <sup>15</sup>N enrichment over time. The <sup>15</sup>N enrichment of the N<sub>2</sub>O molecule, over time, is shown for N<sub>2</sub>O evolved from soil under near saturated (−1 kPa) or field capacity (−10 kPa) conditions, following <sup>15</sup>N urea application. Symbols are means (n = 4) with vertical error bars the standard error of the mean.

Upon urea application, the atom % <sup>15</sup>N enrichment of the N<sub>2</sub>O emitted at −1 kPa increased steadily to reach a maximum value of 43.9 atom % <sup>15</sup>N on day 25 before declining at a relatively slow rate to a value of 36.3 atom % <sup>15</sup>N by day 59 (Fig. 7). With the exception of day 2, the atom % <sup>15</sup>N enrichment of the N<sub>2</sub>O emitted at −1 kPa was higher than that emitted at −10 kPa (P < 0.05) on any given day. At −10 kPa the atom % <sup>15</sup>N enrichment of the N<sub>2</sub>O flux was observed to increase abruptly at day 12, reaching a maximum of 32.8 on day 30 and thereafter declining relatively abruptly to remain at ca 10 atom % <sup>15</sup>N (Fig. 7). Fluxes of N<sub>2</sub>O associated with codenitrification were low and only measurable on days 2, 5, 8 and 12 for the −1 kPa treatment and days 3, 5, 8, 12 and 16 for the −10 kPa treatment (Fig. 8). Highest fluxes were observed for the −1 kPa treatment (3637 μg N<sub>2</sub>O-N m<sup>-2</sup> hr<sup>-1</sup>) comprising 20% of total N<sub>2</sub>O flux with emissions of codenitrified N<sub>2</sub>O subsequently reducing rapidly. Codenitrified N<sub>2</sub>O fluxes in the −10 kPa treatment were extremely low and never rose above 70 μg N<sub>2</sub>O-N m<sup>-2</sup> hr<sup>-1</sup>).

**N<sub>2</sub> fluxes and codenitrification after urea addition.** The average daily denitrification fluxes were 1.48 (0.34) g N m<sup>-2</sup> d<sup>-1</sup> and 0.53 (0.07) g m<sup>-2</sup> d<sup>-1</sup> (s.e.m in brackets) at −1 and −10 kPa, respectively. At −1 kPa denitrification fluxes initially peaked at day 5 and then were higher after day 30, peaking on day 49 (Fig. 8). The decline in soil NO<sub>3</sub><sup>-</sup> concentration after day 35 coincided with higher denitrification fluxes. At −10 kPa denitrification fluxes were highest after the initial wetting up following treatment application where after they generally declined (Fig. 8). Consequently, cumulative denitrification as N<sub>2</sub> was higher (p = 0.055) at −1 kPa, totaling 8.61 g N m<sup>-2</sup>, than at −10 kPa where observed fluxes were 1.98 g N m<sup>-2</sup> (Fig. 8).

The average daily codenitrification fluxes under urea treatments at −1 and −10 kPa were 0.38 (0.15) g N m<sup>-2</sup> d<sup>-1</sup> and −10 kPa 0.07 (0.01) g N m<sup>-2</sup> d<sup>-1</sup>, respectively. Codenitrification fluxes peaked on day 12 regardless of soil kPa value, but were higher on day 10 at −1 kPa (Fig. 8). Average daily codenitrification fluxes were ca 5-fold higher at −1 kPa after day 30 than at −10 kPa. Consequently, cumulative codenitrification rates of N<sub>2</sub> were also higher (p = 0.043) at −1 kPa (1.91 g N m<sup>-2</sup>) than at −10 kPa (0.26 g N m<sup>-2</sup>). Cumulative codenitrification, as a proportion of denitrification, did not vary as a result of soil matric potential equaling 25.5 ± 15.8% and 12.9 ± 4.8% (±stdev) at −1 and −10 kPa, respectively. The contribution of codenitrification as a proportion of total denitrification (codenitrification plus denitrification) also did not vary with soil matric potential, being 19.3 ± 10.4% and 11.3 ± 3.8% (±stdev) at −1 and −10 kPa, respectively.

## Discussion

**Inorganic-N pools and <sup>15</sup>N enrichment.** Following urea application to the soil the ensuing hydrolysis produces NH<sub>4</sub><sup>+</sup> and bicarbonate (HCO<sub>3</sub><sup>-</sup>) ions. The HCO<sub>3</sub><sup>-</sup> ions are further hydrolysed to produce hydroxide ions (OH<sup>-</sup>) and carbon dioxide<sup>25</sup> and it is this second hydrolysis reaction that generated the observed increase in soil pH under the urea treatments (Fig. 2). Elevated soil pH also influences the equilibrium between NH<sub>4</sub><sup>+</sup> and ammonia (NH<sub>3</sub>): as soil pH becomes elevated (>7.0) concentrations of NH<sub>3</sub> increase<sup>25</sup>. Urea-N not volatilized as NH<sub>3</sub> may be transferred along the inorganic-N cascade via NH<sub>4</sub><sup>+</sup>, NO<sub>2</sub><sup>-</sup> and NO<sub>3</sub><sup>-</sup>.

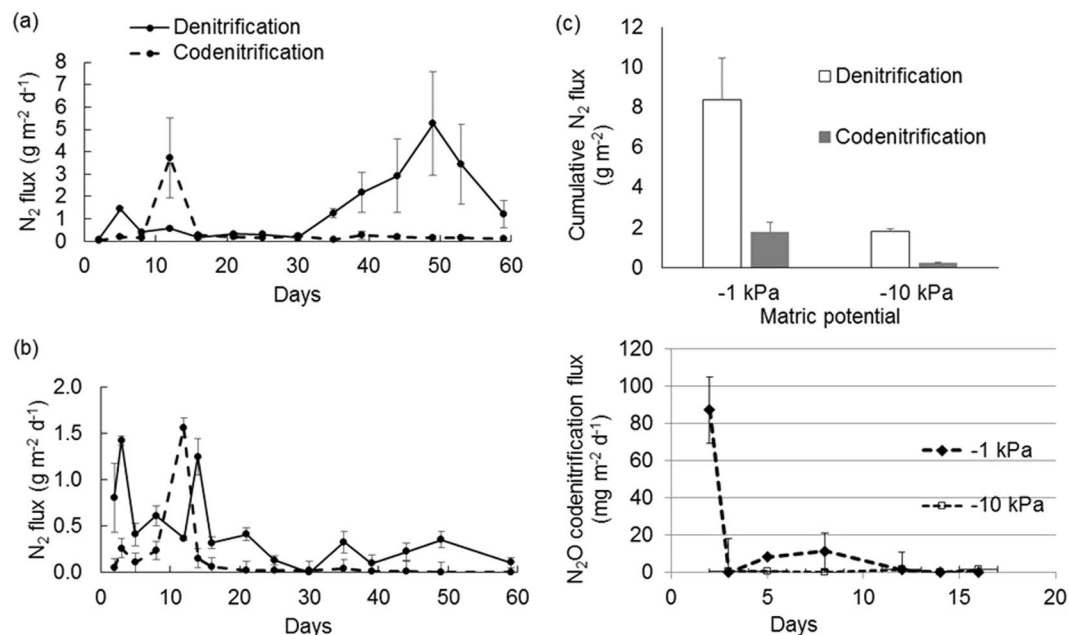


**Figure 8.** Denitrification and codenitrification fluxes over time. The codenitrification and denitrification fluxes, over time since <sup>15</sup>N urea addition, are shown as daily N<sub>2</sub> fluxes for (a) soil at -1 kPa (b) soil at -10 kPa and (c) as cumulative codenitrification and denitrification N<sub>2</sub> fluxes, while (d) is the N<sub>2</sub>O codenitrification flux, over time since <sup>15</sup>N urea addition, as daily N<sub>2</sub>O fluxes. Symbols are means (n = 4) with vertical error bars the standard error of the mean.

During nitrification microbes utilise NH<sub>4</sub><sup>+</sup> and oxidise it to NO<sub>2</sub><sup>-</sup>. Elevated NH<sub>3</sub> concentrations may inhibit NH<sub>4</sub><sup>+</sup> oxidation<sup>26, 27</sup>. Thus the slower decline in the NH<sub>4</sub><sup>+</sup> concentration observed in the -10 kPa treatment, under urea, may have been due to NH<sub>3</sub> inhibition of nitrification. In favour of this were both the relative gas diffusivity of the soil being 2 orders of magnitude higher at -10 kPa, which would have facilitated NH<sub>3</sub> diffusion through the soil, and the soil pH remaining higher for longer (Fig. 2). The latter would have promoted the presence of NH<sub>3</sub> for longer. A slower rate of decline in soil pH at -10 kPa also demonstrates nitrification was slower, since nitrification results in the net release of H<sup>+</sup> ions<sup>19</sup>. Further evidence to support a slower rate of NH<sub>4</sub><sup>+</sup> oxidation can be found in the slower rate of increase in ammonium oxidizing bacteria (AOB) gene and transcript abundance<sup>28</sup>.

Elevated soil NO<sub>2</sub><sup>-</sup> concentrations resulted from nitrification of NH<sub>4</sub><sup>+</sup> and their increase, from day 5 until day 20, occurred over a period when soil pH was sufficiently high to result in NH<sub>3</sub> generation. Ammonia toxicity acts more strongly on nitrifier NO<sub>2</sub><sup>-</sup> oxidation than nitrifier NH<sub>4</sub><sup>+</sup> oxidation<sup>29</sup>. It has been shown that solution-phase NH<sub>3</sub> (*s*/NH<sub>3</sub>) inhibits NO<sub>2</sub><sup>-</sup> oxidation, as evidenced by strong relationships between cumulative *s*/NH<sub>3</sub> and cumulative NO<sub>2</sub><sup>-</sup> and static copy numbers of the *nxrA* gene, which is associated with nitrite oxidoreductase, and as a consequence soil NO<sub>2</sub><sup>-</sup> is strongly correlated with N<sub>2</sub>O production<sup>29</sup>. The high N<sub>2</sub>O fluxes that occurred, between ca. days 7 to 35, at both -1 and -10 kPa under urea, where the soil NO<sub>2</sub><sup>-</sup> concentrations were elevated strongly demonstrates this, and it can be assumed *s*/NH<sub>3</sub> induced NO<sub>2</sub><sup>-</sup> toxicity lead to the ensuing N<sub>2</sub>O emissions.

The higher NO<sub>3</sub><sup>-</sup> concentrations observed under urea on days 14 and 21 at -1 kPa were a consequence of the more rapid nitrification rates in this treatment, while the lower NO<sub>3</sub><sup>-</sup> concentration in this treatment observed at day 63 resulted from higher denitrification induced losses of NO<sub>3</sub><sup>-</sup>, which is further supported by the increase in soil pH under this treatment, since denitrification results in a net release of OH<sup>-</sup> ions<sup>19</sup>.

The <sup>15</sup>N enrichment of the NH<sub>4</sub><sup>+</sup> pool, under urea, shows that it was predominantly derived from the urea applied, regardless of soil moisture treatment. The fact the NH<sub>4</sub><sup>+</sup> pool <sup>15</sup>N enrichment was initially ca. 5 atom% lower than the urea solution applied was likely due to the release of NH<sub>4</sub><sup>+</sup> as a consequence of the high soil pH solubilising soil organic matter, as demonstrated by the elevated DOC concentrations under the urea treatment. Solubilisation of soil organic matter is routinely observed following urine or urea application to soil<sup>30</sup>. The reason for the NO<sub>2</sub><sup>-</sup> pool <sup>15</sup>N enrichment being ca. half that observed in the NH<sub>4</sub><sup>+</sup> pool on days 14 and 21 at -1 kPa, shows antecedent soil N was also contributing to this pool which could have come from mineralization and subsequent oxidation of NH<sub>4</sub><sup>+</sup>, despite the presence of NH<sub>3</sub>, since relatively low quantities of NH<sub>4</sub><sup>+</sup> would be needed to dilute the NO<sub>2</sub><sup>-</sup> pool, or alternatively there may have been some denitrification of antecedent NO<sub>3</sub><sup>-</sup> generating NO<sub>2</sub><sup>-</sup>. The fact that the NO<sub>3</sub><sup>-</sup> pool <sup>15</sup>N enrichment aligned closely with that of the NO<sub>2</sub><sup>-</sup> pool <sup>15</sup>N enrichment at -10 kPa demonstrates NO<sub>2</sub><sup>-</sup> was the dominant precursor to NO<sub>3</sub><sup>-</sup> pool at -10 kPa. Furthermore, the slower rate of increase in the NO<sub>3</sub><sup>-</sup> pool <sup>15</sup>N enrichment at -10 kPa, when compared to -1 kPa, further supports the fact there was a slower rate of nitrification at -10 kPa. The increase in the NO<sub>3</sub><sup>-</sup> pool <sup>15</sup>N enrichment over time, in both the -1 and -10 kPa treatments, demonstrates the NO<sub>3</sub><sup>-</sup> pool was initially dominated by antecedent soil NO<sub>3</sub><sup>-</sup> as in fact occurred (Fig. 4c).

**N<sub>2</sub>O fluxes and <sup>15</sup>N enrichment.** While simply wetting of the soil, as occurred under the non-urea treatment, induced N<sub>2</sub>O fluxes at −1 kPa, this wetting effect was not sufficient to generate the high N<sub>2</sub>O fluxes observed under urea from days 0 to 4. These high initial N<sub>2</sub>O fluxes under urea, as previously observed<sup>31</sup>, are due to the chemically induced anoxia that results from the hydrolysis reactions generating both NH<sub>3</sub> and CO<sub>2</sub>, as demonstrated *in situ*<sup>32</sup>. Such high fluxes were not observed at −10 kPa during this period because the higher relative gas diffusivity of the soil at −10 kPa ensured the soil was not as anaerobic.

As noted above periods of high N<sub>2</sub>O flux between days 14 and 37 aligned with the presence of elevated NO<sub>2</sub><sup>−</sup> concentrations. The atom % <sup>15</sup>N enrichment of the N<sub>2</sub>O at −10 kPa was comparable with that of the NO<sub>2</sub><sup>−</sup> pool at this time, further demonstrating that the N<sub>2</sub>O flux predominately originated from the NO<sub>2</sub><sup>−</sup> pool, and because the <sup>15</sup>N enrichment of the N<sub>2</sub>O declined as NO<sub>2</sub><sup>−</sup> concentrations declined. Despite both the NO<sub>3</sub><sup>−</sup> concentration and NO<sub>3</sub><sup>−</sup> <sup>15</sup>N enrichment both increasing after this time, this was not reflected in any increased N<sub>2</sub>O fluxes or its <sup>15</sup>N enrichment because the higher relative gas diffusivity at −10 kPa made conditions unsuitable for the denitrification of NO<sub>3</sub><sup>−</sup><sup>24</sup>.

However, at −1 kPa the N<sub>2</sub>O evolved predominately via denitrification of the NO<sub>3</sub><sup>−</sup> pool up until ca. day 15 as demonstrated by the alignment of the N<sub>2</sub>O <sup>15</sup>N enrichment with the NO<sub>3</sub><sup>−</sup> pool <sup>15</sup>N values. The higher N<sub>2</sub>O fluxes at −1 kPa between days 15 to 35 were ca. 15-fold higher due to the more anaerobic conditions and, as inferred above, are presumed to have occurred as a result of the relatively high NO<sub>2</sub><sup>−</sup> concentrations over this period. However, the N<sub>2</sub>O <sup>15</sup>N enrichment did not reflect that of the KCl extracted NO<sub>2</sub><sup>−</sup> pool measured on days 14 and 21 at −1 kPa, but did reflect that of the NH<sub>4</sub><sup>+</sup> and NO<sub>3</sub><sup>−</sup> pools on these days. Differences in the <sup>15</sup>N enrichment of the KCl extracted NO<sub>2</sub><sup>−</sup> and actual *in situ* <sup>15</sup>N enrichment of the NO<sub>2</sub><sup>−</sup> pool may possibly have arisen due to the method of treatment application where, in the −10 kPa treatment the urea solution infiltrated further and contacted a greater soil volume than at −1 kPa, as evidenced by the greater release of DOC at −10 kPa (Fig. 3), and which would have resulted in a more uniform NO<sub>2</sub><sup>−</sup> pool. It is likely that, at −1 kPa, denitrification of antecedent NO<sub>3</sub><sup>−</sup> occurred and that this generated sufficient NO<sub>2</sub><sup>−</sup> to isotopically dilute the relatively small <sup>15</sup>N enriched NO<sub>2</sub><sup>−</sup> pool, derived from NH<sub>4</sub><sup>+</sup> and/or NO<sub>3</sub><sup>−</sup>, when the soil was extracted. After day 35, the N<sub>2</sub>O <sup>15</sup>N enrichment reflected that of the NO<sub>3</sub><sup>−</sup> pool, and given the compatible conditions for denitrification, it can be assumed that denitrification of the NO<sub>3</sub><sup>−</sup> pool dominated N<sub>2</sub>O production after day 30, and this assumption is supported by the elevated denitrification flux occurring after this time (Fig. 8).

**N<sub>2</sub> denitrification and codenitrification of N<sub>2</sub> and N<sub>2</sub>O.** As expected denitrification occurred at higher rates under the more anaerobic moisture treatment as a result of the lower *Dp/Do* conditions promoting denitrification in the presence of NO<sub>3</sub><sup>−</sup> substrate.

The N transformations that ensued following urea hydrolysis, and hydrolysis itself, generated previously recognized codenitrification nucleophiles that include NH<sub>4</sub><sup>+</sup>, NH<sub>3</sub>, and possibly organic-N compounds such as amines<sup>16</sup>. The latter might occur as a result of the dissolution of soil organic matter. While the enzymatically utilized NO<sub>2</sub><sup>−</sup> and NO compounds, that form electrophiles, are generated during nitrification and denitrification<sup>19</sup>.

Codenitrification N<sub>2</sub>O fluxes were generally low for both treatments, with measurable values mainly associated with the initial soil wetting. Conversely, codenitrification to N<sub>2</sub> was observed to peak on day 12, regardless of soil moisture, when NH<sub>3</sub>, NH<sub>4</sub><sup>+</sup> and NO<sub>2</sub><sup>−</sup> were all present at an elevated soil pH (≥7.70), and at relatively high concentrations. Thus it is possible that either NH<sub>3</sub> or NH<sub>4</sub><sup>+</sup> were undertaking the role of the nucleophile at this time, since the elevated pH (>5.5) would have prevented any significant abiotic nitrosation occurring via NO<sup>+</sup> formation<sup>16</sup>. Recently, however, the formation of both N<sub>2</sub>O and N<sub>2</sub>, under both oxic and anoxic conditions, was reported in an *in vitro* experiment maintained at pH 6.2–6.9 where either live fungi or fungal necromass were incubated with glutamine and NO<sub>2</sub><sup>−</sup><sup>33</sup>. A subsequent isotope experiment with glutamine and <sup>15</sup>NO<sub>2</sub><sup>−</sup> demonstrated the hybrid formation of N<sub>2</sub> after an incubation period of >7 days, again under either oxic or anoxic conditions<sup>33</sup>. Hence, based on this recent study, even though the soil in the current study was at a pH (≥7.70) sufficient to prevent acidic pathways of abiotic hybrid N-N bonds forming, we cannot rule out the possibility that abiotic reactions, under alkaline conditions, contributed to the codenitrification flux measured in the current experiment.

Production of N<sub>2</sub>O or N<sub>2</sub> via biotic codenitrification may result from the actions of archaea, bacteria or fungi. While archaea have been found to generate N<sub>2</sub>O through N-nitrosating hybrid formation<sup>34</sup> they are unlikely to have been the dominant mechanism in the current study since archaea are thought to prefer low N conditions<sup>35, 36</sup> and urea addition resulted in lower ammonia oxidizing archaea gene copy numbers<sup>28</sup>. The codenitrification observed is most likely to be the result of fungi or bacterial activity. Delineation of the relative contributions made by fungi or bacteria to codenitrification is beyond the scope of the present study, however, future studies should aim to examine relative fungal and bacterial contributions.

Spott *et al.*<sup>16</sup> conceptualized that the recognized constraints on denitrification might also apply to codenitrification, and thus higher codenitrification fluxes might be expected under more anaerobic conditions. The current results support this concept: after day 30 the higher daily codenitrification fluxes under the more anaerobic (−1 kPa) soil moisture conditions, when at the same time denitrification fluxes were higher, resulted in higher cumulative codenitrification fluxes. This reinforces the fact that NO<sub>2</sub><sup>−</sup> and or NO play a key role in the codenitrification process. The NO molecule has been observed to readily diffuse within the soil profile<sup>37</sup>, at relatively high concentrations, during denitrification and this would result in reactions with nucleophiles.

Unlike the results of Selbie *et al.*<sup>23</sup> codenitrification did not dominate the N<sub>2</sub> fluxes observed in the current study. This could be the result of the experimental system used in the current study differing to that used by Selbie *et al.*<sup>23</sup>. Differences include the lack of a pasture turf and associated microbiology and root exudation, the use of sieved repacked soil that may also have altered the fungal-bacterial community structure or activity as a result of sieving, constant soil moisture contents as opposed to wetting and drying events, and the lack of other climatic variables such as wind and rainfall.



Depth	Bulk density (Mg m <sup>-3</sup> )	Porosity (%)	Texture	Sand (%)	Silt (%)	Clay (%)
0–10	1.19	0.55	Sandy loam	53	31	16
10–20	1.28	0.52	Sandy loam	55	31	14

**Table 2.** Physical and textural characteristics of soil sampled.

In particular, fungal populations may have been reduced on sieving, and given that fungal P450 NOR is implicated in supplying enzyme bound nitrosating agents this could have had a significant influence on the results<sup>38</sup>. Given that enzyme bound nitrosating agents produced during denitrification may also consist of metal-nitrosyl complexes<sup>16</sup> any differences in soil Fe and Cu levels between studies may also explain the observed differences in codenitrification. Likewise, differences in the kinetic properties of different nucleophiles, combined with the ratio of NO or NO<sub>2</sub><sup>-</sup> availability to nucleophile concentration, have also been shown to significantly impact on codenitrification/denitrification: lower  $K_m$ , and high nitrosyl donor/nucleophile ratios have been shown to reduce the level of codenitrification<sup>15,20</sup>.

This study confirms the role of anaerobic soil conditions in enhancing codenitrification fluxes under ruminant urine/urea deposition. It also demonstrates for the first time that high levels of NO<sub>2</sub><sup>-</sup>, or other transitional N compounds ensuing from NO<sub>2</sub><sup>-</sup>, that may occur during nitrification, are also able to contribute to codenitrification processes. To progress knowledge of codenitrification in grazed pastures more detailed studies are now required to both identify the microbial pathways operating and the relative importance of the possible nucleophiles and nitrosating agents that occur in grazed pastures.

## Materials and Methods

**Soil collection and experimental design.** Soil was collected in early spring (March) from a permanently grazed dairy pasture at the Teagasc Moorepark Research Centre, County Cork, Ireland (8°15'W, 52°9'N). The top 5 cm of soil was removed and the A-horizon was sampled, 5–20 cm depth. Soil physical and textural characteristics are shown in Table 2. Cows had not grazed the pasture for over one month so recent urine deposition sites were avoided. The soil is classified as a Typical Brown earth from the Clashmore Series<sup>39</sup>, or as a Haplic Cambisol in the World Reference Database<sup>40</sup>. Field moist soil was then bagged and shipped to Lincoln University, New Zealand, following appropriate biosecurity protocols. It was then sieved ( $\leq 2$  mm) to remove any stones, plant roots or earthworms. Sieved soil, with a gravimetric water content ( $\theta_g$ ) of 0.24 g water g<sup>-1</sup> soil, was then packed into stainless steel rings (7.3 cm internal diameter, 7.4 cm deep) to a depth of 4.1 cm at a bulk density of 1.1 Mg m<sup>-3</sup>, the latter simulating the *in situ* soil bulk density. This resulted in a total porosity of 0.58 cm<sup>3</sup> pores cm<sup>-3</sup> soil. Packed soil cores were then arranged in a factorial experiment replicated four times.

Treatments consisted of two levels of soil moisture,  $-1$  kPa and  $-10$  kPa simulating 'near-saturation' and 'field-capacity', respectively, and two levels of urea, (0 and 1000 kg N ha<sup>-1</sup>), replicated 4 times, with 7 destructive sampling times (112 cores in total). Preliminary tests showed that  $-1$  and  $-10$  kPa corresponded to 53% and 30% volumetric water content, or 91% and 52% water-filled pore space (WFPS). Soil cores were maintained at these water contents using tension tables<sup>41</sup>. Soil relative gas diffusivity values were calculated using the values for air-filled pore space and total porosity and the generalized-density corrected equation of Chamindu Deepagoda *et al.*<sup>42</sup>; Equation 9b. It is recognized that artificial urine simulation does not generate identical effects to ruminant urine<sup>43</sup>, that urea contributes  $>70\%$  of the total urine-N pool<sup>6,44</sup>, and that this N source is predominately responsible for the subsequent dynamics and transformations of organic and inorganic N in the soil under ruminant urine patches. Thus, in order to apply the N treatments, soil cores were wetted up on the tension tables to a point where there remained the capacity to add a further 10 mL of liquid, without inducing drainage. Subsequently, in the plus N treatment, 10 mL of a urea solution (42 g urea-N L<sup>-1</sup>; 50 atom%, Cambridge Isotope Laboratories Inc., USA) was slowly applied to the soil surface, to avoid drainage, to mimic an extreme bovine urine deposition event with a potentially high N<sub>2</sub> flux. Real urine could not be used since there was a need to have the urea-N highly enriched with <sup>15</sup>N to detect N<sub>2</sub> fluxes. In the nil N treatment 10 mL of deionized water was applied instead of a urea solution. Tension tables were maintained in a room with a mean temperature of 20 °C.

**Soil chemical analyses.** After treatment application and throughout the experiment, on days 0, 3, 7, 14, 21, 35, and 63, soil inorganic N concentrations were determined by destructively sampling 16 soil cores (2 levels of urea  $\times$  two levels of soil moisture  $\times$  4 replicates). Soil cores were fully extracted, homogenized, and a subsample was taken to determine  $\theta_g$ : by drying the soil at 105 °C for 24 hours. A flat surface pH electrode was used to determine soil pH (Broadley James Corp., Irvine, California). Then further soil subsamples were extracted (equivalent of 10 g dry soil: 100 mL 2 M KCl shaken for 1 hour) and filtered (Whatman 42) to determine soil inorganic-N. The NH<sub>4</sub><sup>+</sup>-N, NO<sub>2</sub><sup>-</sup>-N, and NO<sub>3</sub><sup>-</sup>-N concentrations were analysed using flow injection analysis<sup>45</sup>. The <sup>15</sup>N enrichment of NH<sub>4</sub><sup>+</sup>-N was determined according to Stark and Hart<sup>46</sup> while NO<sub>2</sub><sup>-</sup>-<sup>15</sup>N and NO<sub>3</sub><sup>-</sup>-<sup>15</sup>N enrichments were determined according to the methods of Stevens and Laughlin<sup>47</sup>. Concentrations of dissolved organic carbon (DOC) in the soil were measured according to Ghani *et al.*<sup>48</sup> with analyses performed on a Shimadzu TOC analyzer (Shimadzu Oceania Ltd., Sydney, Australia).

**Gas flux determinations.** Nitrous oxide and N<sub>2</sub> fluxes were regularly determined, from two days before until 63 days after treatment application using only the last batch of soil cores to be destructively analysed. This was performed by placing a soil core into a 1-L stainless steel tin fitted with a gas-tight lid and rubber septa. Samples for N<sub>2</sub>O flux determinations were taken upon lid closure and then after 15 and 30 minutes. A further sample

was taken for  $N_2O$ - $^{15}N$  enrichment and  $N_2$  flux determination after 3 hours, after which cores were returned to the tension tables. Gas samples were taken using a 20-mL glass syringe fitted with a 3-way tap and a 0.5 mm by 16 mm needle and placed in either 6 mL vials for the  $N_2O$  flux determinations or 12 mL vials for the  $N_2O$ - $^{15}N$  enrichment and  $N_2$  flux samples (Exetainer; Labco Ltd., Lampeter, UK). An automated gas chromatograph (8610; SRI Instruments, Torrance, CA), coupled to an autosampler (Gilson 222XL; Gilson, Middleton, WI), was used to determine  $N_2O$  gas concentrations in the samples, as previously described<sup>49</sup>. A continuous-flow-isotope mass spectrometer (Sercon 20/20; Sercon, Chesire, UK) inter-faced with a TGII cryofocusing unit (Sercon, Chesire, UK), was used to determine the  $^{15}N$  enrichment of the  $N_2O$ -N and  $N_2$ -N gas samples<sup>50</sup>.

The ion currents (I) at mass to charge ratios (m/z) of 44, 45, and 46 facilitated the calculation of the  $N_2O$  molecular mass ratios  $^{45}R$  ( $^{45}I/^{44}I$ ) and  $^{46}R$  ( $^{46}I/^{44}I$ ). The  $N_2O$  sources were subsequently allocated to either the fraction derived from the denitrifying pool ( $d'_D$ ) of enrichment  $aD$  or the fraction derived from the pool or pools at natural abundance  $d'_N = (1 - d'_D)$  using the method of Arah (1997). The ion currents at m/z 28, 29, and 30 permitted the  $N_2$  molecular ratios  $^{29}R$  ( $^{29}I/^{28}I$ ) and  $^{30}R$  ( $^{30}I/^{28}I$ ) to be quantified. Differences between the  $N_2$  molecular ratios of the enriched and ambient atmospheres were expressed as  $\Delta^{29}R$  and  $\Delta^{30}R$ . The  $N_2$  flux was subsequently calculated using three methods:

- (i) The enrichment of the denitrifying pool ( $^{15}X_N$ ) was calculated using  $\Delta^{29}R$  and  $\Delta^{30}R$ , and then the  $N_2$  flux<sup>51</sup>,
- (ii) Using only the  $\Delta^{30}R$  data with the assumption that the enrichment of the denitrifying pool was  $aD$ <sup>52</sup> and the equation of Mulvaney<sup>53</sup>
- (iii) Using  $\Delta^{29}R$  and  $\Delta^{30}R$  to calculate the relative contributions of denitrification ( $N_{2DN}$ ), according to method (ii), and codenitrification ( $N_{2CO}$ ).

Increases in  $\Delta^{29}R$  and  $\Delta^{30}R$  may occur from denitrification but codenitrification contributes most to  $\Delta^{29}R$  where the ratio of  $\Delta^{29}R$  to  $\Delta^{30}R$  is always 272<sup>54</sup>. By assuming all  $\Delta^{30}R$  was the result of denitrification, method (ii),  $N_{2DN}$  was calculated. Then using the 'backsolver' facility in Microsoft Excel<sup>TM</sup>, the contribution of  $\Delta^{29}R$  to  $N_{2DN}$  was determined. The difference between the total measured value of  $\Delta^{29}R$  and  $\Delta^{29}R$  determined for  $N_{2DN}$  was assigned to codenitrification. Thus the fraction of the total number of moles of  $N_2$  in the headspace, resulting from codenitrification ( $d_{CD}$ ) were calculated as:

$$d_{CD} = -\Delta^{29}Rp_1^2 / (-\Delta^{29}Rp_1^2 + \Delta^{29}Rp_1p_2 + q_1p_2 - q_2p_1) \quad (1)$$

where  $p_1$  (0.9963) and  $q_1$  (0.0037) represent the atom fractions of  $^{14}N$  and  $^{15}N$  in the natural abundance pool, respectively, and  $p_2$  and  $q_2$  are the atom fractions of  $^{14}N$  and  $^{15}N$  in the enriched  $NO_3^-$  pool, respectively, from which codenitrification is assumed to occur. Using the headspace volume of the sample chamber, corrected for standard temperature and pressure, the mass of  $N_2$ -N in the headspace was determined with the amount derived from denitrification or codenitrification ascertained by multiplying by  $d_D$  or  $d_{CD}$ , respectively.

**Data analyses.** Data were analysed using the Glimmix procedure within the SAS<sup>®</sup> software version 9.4 (SAS, 2014). Cumulative results were analysed for the +N treatment only. For all other variables, analyses was as N treatment  $\times$  moisture  $\times$  day or moisture  $\times$  day factorials. Any repeated measurements over time were modelled using correlation structures and spatial covariance was used to model the unequally-spaced time measurements. Residual checks were made and, where required, log transformation was used to correct for skew and non-constant variance. Multiplicity adjustments were made for simple effects within interactions, as interest was primarily in comparisons within time points.

## References

1. IPCC, Summary for Policymakers. In *Climate Change 2013: The Physical Science Basis. Contribution of Working Group I to the Fifth Assessment Report of the Intergovernmental Panel on Climate Change*, edited by Stocker, T. F. *et al.*, pp. 1535 (Cambridge University Press, 2013).
2. Ravishankara, A. R., Daniel, J. S. & Portmann, R. W. Nitrous Oxide ( $N_2O$ ): The Dominant Ozone-Depleting Substance Emitted in the 21st Century. *Science* **326**, 123–125, doi:10.1126/science.1176985 (2009).
3. Ciais, P. *et al.* Carbon and Other Biogeochemical Cycles. In: *Climate Change 2013: The Physical Science Basis. Contribution of Working Group I to the Fifth Assessment Report of the Intergovernmental Panel on Climate Change*. (Cambridge University Press, Cambridge, United Kingdom, 2013).
4. Hargreaves, P. R., Rees, R. M., Horgan, G. W. & Ball, B. C. Size and Persistence of Nitrous Oxide Hot-Spots in Grazed and Ungrazed Grassland. *Environ. Nat. Resour. Res.* **5**(4), 1, doi:10.5539/enrr.v5n4p1 (2015).
5. Oenema, O. *et al.* Trends in global nitrous oxide emissions from animal production systems. *Nutr. Cycl. Agroecosyst.* **72**(1), 51–65, doi:10.1007/s10705-004-7354-2 (2005).
6. Haynes, R. J. & Williams, P. H. Nutrient cycling and soil fertility in the grazed pasture ecosystem. *Adv. Agron.* **49**, 119–199, doi:10.1016/S0065-2113(08)60794-4 (1993).
7. Selbie, D. R., Buckthought, L. E. & Shepherd, M. A. The Challenge of the Urine Patch for Managing Nitrogen in Grazed Pasture Systems. *Adv. Agron.* **129**, 229–292, doi:10.1016/bs.agron.2014.09.004 (2015).
8. Zhu, X., Burger, M., Doaneb, T. A. & Howarth, W. R. Ammonia oxidation pathways and nitrifier denitrification are significant sources of  $N_2O$  and NO under low oxygen availability. *P Natl. Acad. Sci. USA* **110**(16), 6328–6333, doi:10.1073/pnas.1219993110 (2013).
9. Laughlin, R. J. & Stevens, R. J. Evidence for fungal dominance of denitrification and codenitrification in a grassland soil. *Soil Sci. Soc. Am. J.* **66**(5), 1540–1548, doi:10.2136/sssaj2002.1540 (2002).
10. Firestone, M. K. & Davidson, E. A. Microbiological Basis of NO and  $N_2O$  Production and Consumption in Soil In *Exchange of Trace Gases between Terrestrial Ecosystems and the Atmosphere*, edited by Andreae, M. O. & Schimel, D. S., pp. 7–21 (John Wiley & Sons Ltd, New York, 1989).
11. Allison, F. E. The enigma of soil nitrogen balance sheets. *Adv. Agron.* **7**, 213–250, doi:10.1016/S0065-2113(08)60339-9 (1955).
12. Clough, T. J. *et al.* Resolution of the N-15 balance enigma? *Aust. J. Soil Res.* **39**(6), 1419–1431, doi:10.1071/SR00092 (2001).

13. Ball, R., Keeney, D. R., Theobald, P. W. & Nes, P. Nitrogen balance in urine-affected areas of a New Zealand pasture. *Agron. J* **71**, 309–314, doi:10.2134/agronj1979.00021962007100020022x (1979).
14. Shoun, H., Kim, D. H., Uchiyama, H. & Sugiyama, J. Denitrification by fungi. *FEMS Microbiol. Lett.* **94**, 277–281, doi:10.1111/fml.1992.94.issue-3 (1992).
15. Tanimoto, T., Hatano, K., Kim, D. H., Uchiyama, H. & Shoun, H. Co-denitrification by the denitrifying system of the fungus *Fusarium oxysporum*. *FEMS Microbiol. Lett.* **93**, 177–180, doi:10.1111/fml.1992.93.issue-2 (1992).
16. Spott, O., Russow, R. & Stange, C. F. Formation of hybrid N<sub>2</sub>O and hybrid N<sub>2</sub> due to codenitrification: First review of a barely considered process of microbially mediated N-nitrosation. *Soil Biol. Biochem.* **43**, 1995–2011, doi:10.1016/j.soilbio.2011.06.014 (2011).
17. Baggs, E. M. & Philippot, L. Microbial terrestrial pathways to nitrous oxide. In *Nitrous Oxide and Climate Change* (Earthscan, 2010).
18. Weeg-Aeressens, E., Tiedje, J. M. & Averill, B. A. Evidence from isotope labeling studies for a sequential mechanism for dissimilatory nitrite reduction. *J. Am. Chem. Soc.* **110**, 6851–6856 (1988).
19. Wrage, N., Velthof, G. L., van Beusichem, M. L. & Oenema, O. Role of nitrifier denitrification in the production of nitrous oxide. *Soil Biol. Biochem.* **33**, 1723–1732, doi:10.1016/S0038-0717(01)00096-7 (2001).
20. Kim, C. H. & Hollocher, T. C. Catalysis of nitrosyl transfer-reactions by a dissimilatory nitrite reductase (cytochrome-cd1). *J. Biol. Chem.* **259**, 2092–2099 (1984).
21. Van Cleemput, O. & Samater, A. H. Nitrite in soils: accumulation and role in the formation of gaseous N compounds. *Fert. Res.* **45**, 81–89, doi:10.1007/BF00749884 (1996).
22. Sen, S. & Chalk, P. M. Chemical interactions between soil N and alkaline-hydrolysing N fertilizers. *Fert. Res.* **36**, 239–248, doi:10.1007/BF00748702 (1993).
23. Selbie, D. R. *et al.* Confirmation of co-denitrification in grazed grassland. *Scientific Reports* **5**, Article number: 17361 (2015).
24. Balaine, N., Clough, T. J., Beare, M. H., Thomas, S. M. & Meenken, E. D. Soil Gas Diffusivity Controls N<sub>2</sub>O and N<sub>2</sub> Emissions and their Ratio. *Soil Sci. Soc. Am. J.* (2016).
25. Avnimelech, Y. & Laher, M. Ammonia volatilization from soils: Equilibrium considerations. *Soil Sci. Soc. Am. J.* **41**, 1080–1084, doi:10.2136/sssaj1977.03615995004100060013x (1977).
26. Anthonisen, A. C., Loehr, R. C., Prakasam, T. B. S. & Srinath, E. G. Inhibition of nitrification by ammonia and nitrous acid. *J. Water Pollut. Control Fed.* **48**, 835–852 (1976).
27. Park, S. & Bae, W. Modeling kinetics of ammonium oxidation and nitrite oxidation under simultaneous inhibition by free ammonia and free nitrous acid. *Proc. Biochem.* **44**, 631–640, doi:10.1016/j.procbio.2009.02.002 (2009).
28. Samad, M. S. *et al.* Response to nitrogen addition reveals metabolic and ecological strategies of soil bacteria. *bioRxiv* (107961) (2017).
29. Venterea, R., Clough, T. J., Coulter, J. A. & Breuillin-Sessoms, F. Ammonium sorption and ammonia inhibition of nitrite-oxidizing bacteria explain contrasting soil N<sub>2</sub>O production. *Science Reports* **5**, 12153, doi:10.1038/srep12153 (2015).
30. Clough, T. J. *et al.* The mitigation potential of hippuric acid on N<sub>2</sub>O emissions from urine patches: An *in situ* determination of its effect. *Soil Biol. Biochem.* **41**, 2222–2229, doi:10.1016/j.soilbio.2009.07.032 (2009).
31. Krol, D. J., Forrester, P. J., Lanigan, G. J. & Richards, K. G. *In situ* N<sub>2</sub>O emissions are not mitigated by hippuric and benzoic acids under denitrifying conditions. *Sci. Total Environ* **511**, 362–368, doi:10.1016/j.scitotenv.2014.12.074 (2015).
32. Owens, J. *et al.* Nitrous Oxide Fluxes, Soil Oxygen, and Denitrification Potential of Urine- and Non-Urine-Treated Soil under Different Irrigation Frequencies. *J. Environ. Qual.* **45**(4), 1169–1177, doi:10.2134/jeq2015.10.0516 (2016).
33. Phillips, R. L. *et al.* Chemical formation of hybrid di-nitrogen calls fungal codenitrification into question. *Scientific Reports* **6**, 39077, doi:10.1038/srep39077 (2016).
34. Stieglmeier, M. *et al.* Aerobic nitrous oxide production through N-nitrosating hybrid formation in ammonia-oxidizing archaea. *ISME J.* **8**, 1135–1146, doi:10.1038/ismej.2013.220 (2014).
35. Di, H. J. *et al.* Nitrification driven by bacteria and not archaea in nitrogen-rich grassland soils. *Nat. Geosci.* **2**, 621–624, doi:10.1038/ngeo613 (2009).
36. Sterngren, A. E., Hallin, S. & Bengtson, P. Archaeal Ammonia Oxidizers Dominate in Numbers, but Bacteria Drive Gross Nitrification in N-amended Grassland Soil. *Front. Microbiol.* **6**, doi:10.3389/fmicb.2015.01350, Article Number 1350 (2015).
37. Clough, T. J., Rolston, D. E., Stevens, R. J. & Laughlin, R. J. N<sub>2</sub>O and N<sub>2</sub> gas fluxes, soil gas pressures, and ebullition events following irrigation of <sup>15</sup>NO<sub>3</sub><sup>-</sup>-labelled subsoils. *Aust. J. Soil Res.* **41**(3), 401–420, doi:10.1071/SR02104 (2003).
38. Wasser, I. M., de Vries, S., Moenne-Loccoz, P., Schroder, I. & Karlin, K. D. Nitric oxide in biological denitrification: Fe/Cu metalloenzyme and metal complex NOX redox chemistry. *Chem. Rev.* **102**, 1201–1234, doi:10.1021/cr0006627 (2002).
39. Gardiner, M. J. & Radford, T. Soil Associations of Ireland and Their Land Use Potential – Explanatory Bulletin to Soil Map of Ireland 1980 (The Agricultural Institute, Dublin, 1980).
40. WRB, IUSS Working Group WRB. 2006. World reference base for soil resources 2006. (Rome, 2006).
41. Romano, N., Hopmans, J. W. & Dane, G. H. Water retention and storage. In *Methods of Soil Analysis, Part 4, Physical Methods*, edited by G. C. Topp & G. H. Dane, pp. 692–698 (Soil Science Society of America, Madison, WI, 2002).
42. Chamindu Deepagoda, T. K. K. *et al.* Generalized Density-Corrected Model for Gas Diffusivity in Variably Saturated Soils. *Soil Sci. Soc. Am. J.* **75**(4), 1315–1329, doi:10.2136/sssaj2010.0405 (2011).
43. Kool, D. M., Hoffland, E., Abrahamse, S. P. A. & van Groenigen, J. W. What artificial urine composition is adequate for simulating soil N<sub>2</sub>O fluxes and mineral N dynamics? *Soil Biol. Biochem.* **38**(7), 1757–1763, doi:10.1016/j.soilbio.2005.11.030 (2006).
44. Bathurst, N. O. The amino acids of sheep and cow urine. *J. Agr. Sci.* **42**, 476–478, doi:10.1017/S0021859600057385 (1952).
45. Blakemore, L. C., Searle, P. L. & Daly, B. K. *Methods for chemical analysis of soils.* (Manaaki-Whenua Press, Lincoln, New Zealand, 1987).
46. Stark, J. M. & Hart, R. H. Diffusion technique for preparing salt solutions, Kjeldahl digests, and persulfate digests for nitrogen-15 analysis. *Soil Sci. Soc. Am. J.* **60**, 1846–1855, doi:10.2136/sssaj1996.03615995006000060033x (1996).
47. Stevens, R. J. & Laughlin, R. J. Determining nitrogen-15 in nitrite or nitrate by producing nitrous oxide. *Soil Sci. Soc. Am. J.* **58**, 1108–1116, doi:10.2136/sssaj1994.03615995005800040015x (1994).
48. Ghani, A., Dexter, M. & Perrott, K. W. Hot-water extractable carbon in soils: a sensitive measurement for determining impacts of fertilisation, grazing and cultivation. *Soil Biol. Biochem.* **35**, 1231–1243, doi:10.1016/S0038-0717(03)00186-X (2003).
49. Clough, T. J., Kelliher, F. M., Wang, Y. P. & Sherlock, R. R. Diffusion of N-15-labelled N<sub>2</sub>O into soil columns: a promising method to examine the fate of N<sub>2</sub>O in subsoils. *Soil Biol. Biochem.* **38**(6), 1462–1468, doi:10.1016/j.soilbio.2005.11.002 (2006).
50. Stevens, R. J., Laughlin, R. J., Atkins, G. J. & Prosser, S. J. Automated determination of nitrogen-15 labelled dinitrogen and nitrous oxide by mass spectrometry. *Soil Sci. Soc. Am. J.* **57**, 981–988, doi:10.2136/sssaj1993.03615995005700040017x (1993).
51. Mulvaney, R. L. & Boast, C. W. Equations for determination of nitrogen-15 labelled dinitrogen and nitrous oxide by mass spectrometry. *Soil Sci. Soc. Am. J.* **50**, 360–363, doi:10.2136/sssaj1986.03615995005000020021x (1986).
52. Stevens, R. J. & Laughlin, R. J. Lowering the detection limit for dinitrogen using the enrichment of nitrous oxide. *Soil Biol. Biochem.* **33**, 1287–1289, doi:10.1016/S0038-0717(01)00036-0 (2001).
53. Mulvaney, R. L. Determination of <sup>15</sup>N-labelled dinitrogen and nitrous oxide with triple-collector mass spectrometers. *Soil Sci. Soc. Am. J.* **48**, 690–692, doi:10.2136/sssaj1984.03615995004800030045x (1984).
54. Clough, T. J., Stevens, R. J., Laughlin, R. J., Sherlock, R. R. & Cameron, K. C. Transformations of inorganic-N in soil leachate under differing storage conditions. *Soil Biol. Biochem.* **33**(11), 1473–1480, doi:10.1016/S0038-0717(01)00056-6 (2001).

55. Schmidt, H. L., Werner, R. A., Yoshida, N. & Well, R. Is the isotopic composition of nitrous oxide an indicator for its origin from nitrification or denitrification? A theoretical approach from referred data and microbiological and enzyme kinetic aspects. *Rapid Commun. Mass Spectrom.* **18**, 2036–2040, doi:10.1002/rcm.1586 (2004).
56. Ye, R. W., Torosuarez, I., Tiedje, J. M. & Averill, B. A. (H<sub>2</sub>O)-O-18 isotope exchange studies on the mechanism of reduction of nitric oxide and nitrite to nitrous oxide by denitrifying bacteria - evidence for an electrophilic nitrosyl during reduction of nitric oxide. *J. Biol. Chem.* **266**, 12848–12851 (1991).

### Acknowledgements

The authors gratefully acknowledge the assistance of Manjula Premaratne and Roger Cresswell in assisting with gas chromatography analyses and mass spectrometer analyses. This work was funded by the New Zealand Government through the New Zealand Fund for Global Partnerships in Livestock Emissions Research to support the objectives of the Livestock Research Group of the Global Research Alliance on Agricultural Greenhouse Gases (Agreement number: 16084) awarded to SEM and the University of Otago. Charlotte Johns gratefully acknowledges funding received from the Teagasc Walsh Fellowship Scheme.

### Author Contributions

C.d.K., K.R. and G.L. were the principal investigators for the project funding. T.C., K.R., G.L. and L.C. designed the experiment. C.J. conducted the measurements. T.C., K.R. and G.L. drafted the manuscript with C.d.K., S.E.M., DR, M.S.S., and L.B. providing assistance with data interpretation and manuscript preparation, while J.G. assisted with statistical interpretation.

### Additional Information

**Competing Interests:** The authors declare that they have no competing interests.

**Publisher's note:** Springer Nature remains neutral with regard to jurisdictional claims in published maps and institutional affiliations.



**Open Access** This article is licensed under a Creative Commons Attribution 4.0 International License, which permits use, sharing, adaptation, distribution and reproduction in any medium or format, as long as you give appropriate credit to the original author(s) and the source, provide a link to the Creative Commons license, and indicate if changes were made. The images or other third party material in this article are included in the article's Creative Commons license, unless indicated otherwise in a credit line to the material. If material is not included in the article's Creative Commons license and your intended use is not permitted by statutory regulation or exceeds the permitted use, you will need to obtain permission directly from the copyright holder. To view a copy of this license, visit <http://creativecommons.org/licenses/by/4.0/>.

© The Author(s) 2017